EXPERIMENTAL INVESTIGATION ON TURBULENT HEAT TRANSFER IN LIQUID METAL ALONG A HEATED ROD IN A VERTICAL ANNULUS

A. Loges¹, T. Baumann¹, L. Marocco², T. Wetzel¹ and R. Stieglitz¹

¹ Karlsruhe Institute of Technology (KIT), Karlsruhe, Germany

² Politecnico di Milano, Milano, Italy
andre.loges@kit.edu

Abstract

In a couple of European research centres, Accelerator Driven Systems (ADS) are investigated for the transmutation of radioactive waste. In one of these concept lead bismuth eutectic (LBE) is applied as coolant. In different experiments covering forced and mixed convection in turbulent LBE flow in a concentric annulus the local velocity and temperature fields were investigated at prototypical power levels and dimensions. Local heat transfer properties were extracted and compared with literature data. A new empirical correlation for the Nusselt number for the thermal entry region for turbulent forced convection in liquid metals is introduced and the transition from forced to mixed convection in LBE is characterized.

Nomenclature

b	aspect ratio	Greek symbols		
c^*	parameter	ρ	density (kg/m ³)	
D	outer radius of annulus (m)	τ	shear stress (N/m ²)	
d_r	inner radius of annulus (m)	v	kinematic viscosity (m ² /s)	
Gr	Grashof number		•	
Gr^*	axial Grashof number	Subscripts		
Nu	Nusselt number	W	wall	
Pr	Prandtl number	wm	mean shear stress on the walls	
Pr_{τ}	turbulent Prandtl number	z	axial position z (m)	
Q	heat flux (W)	∞	thermally developed flow	
q "	heat flux density (W/m ²)			
r	radius [m]			
r*	dimensionless radius			
Pe	Peclet number			
Ra	Rayleigh number			
Ra*	axial Rayleigh number			
Re	Reynolds number			
T	temperature (°C)			
T_{M}	adiabatic mixing temperature (°C)			
T_W	wall temperature (°C)			
и	axial flow velocity (m/s)			
u^{+}	dimensionless axial velocity			
У.	distance from the wall (m)			
y^{+}	dimensionless distance from wall			
Z	parameter			
z	axial distance (m)			
${\mathcal{Z}_h}^*$	dimensionless axial distance			
	referring to the total length of the			
	cylindrical rod			
${z_T}^*$	dimensionless axial distance			
	referring to the heated length			

1. Introduction

Transmutation of minor actinides in an accelerator driven sub-critical system (ADS) is one technical option to reduce radioactive waste and its long-term radiotoxicity.

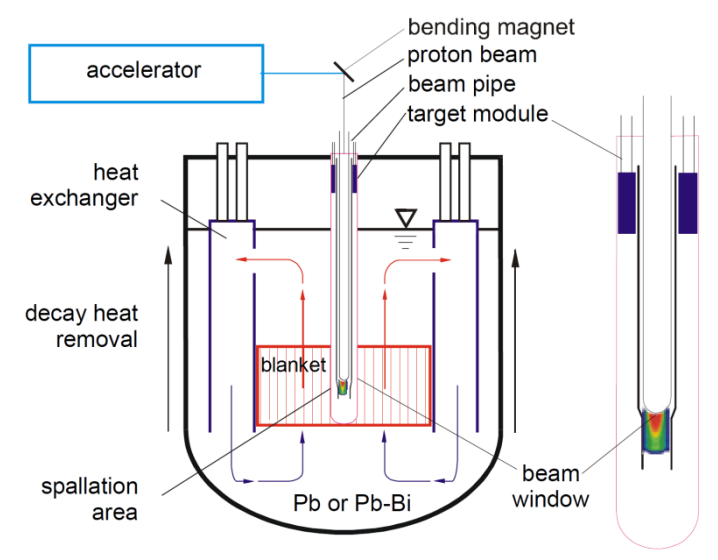


Figure 1: Sketch of ADS

In an ADS, heavy liquid metals (HLM), especially lead bismuth eutectic, have been considered as coolant for both the sub-critical reactor core and the spallation target due to their efficient heat removal properties and high production rate of neutrons (Figure 1) [1,2]. For this reason a generic experimental setup was arranged in KALLA (Karlsruhe Liquid Metal Laboratory) to investigate a turbulent lead bismuth flow facing a single vertical heated rod, concentrically arranged in a circular duct, which represents the basic element of a fuel assembly [3].

Starting from the pioneering works of Martinelli [4] and Lyon [5] still today a large deficiency exists in the basic knowledge of HLM thermal-hydraulics. Reasons may be found in the large scatter between the experimental literature data due to the difficulties in obtaining high quality measurements for these fluids. Moreover only few and old works deal with the thermal entry region for low Prandtl number fluids [6], [7] or with heat transfer to lead-bismuth in pipes [8] or annuli [9].

The turbulent flow of fully developed annular channels has been extensively studied. The experimental works of Rehme for air [10], and Hlavac et al. for mercury [11], the simulations with DNS (Direct Numerical Simulation) by Chung et al. [12], [13] or general analyses by Kaneda et al. [14] can exemplarily be listed.

A detailed summary of the available forced convection correlations for thermally and hydrodynamically fully developed flow in concentric annuli can be found in Kakaç [15]. Detailed studies on forced convection heat transfer in liquid metals are those of Chen and Chiou [6], Dwyer [16] and the theoretical approach to heat transfer in concentric annular flow of Yu et al. [17].

A detailed description of the mixed convection regime, together with many correlations, can be found in Heat Atlas [18]. Aicher and Martin [19] extensively investigated the mixed convective heat transfer for Prandtl numbers ranging from 3 to 4.

In this paper new experimental results from the measurements of the radial and axial turbulent temperature distribution around the heated rod are presented and compared with CFD-simulations (computational fluid dynamics). A new correlation for thermally developing flow in low Prandtl number fluids and a detailed description of the characteristics of buoyancy effects in LBE is obtained. The investigated Reynolds numbers cover the range from $Re=1.48 \times 10^4$ to $Re=2.37 \times 10^5$.

2. Experimental Setup

The set-up of the heated rod experiment conducted in the THESYS2 loop at KALLA is shown in detail in Figure 2. It consists of a traversable and electrically heated cylindrical rod with a sharp tip placed vertically and concentrically in a circular tube (D=60mm). It has a heated section of 860 mm ($0 \le z_T^* \le 16.6$ with $z_T^* = z_T/d_h$, $d_h = (D-d_r)$ and $r^* = (2r-D)/(D-d_r)$) and the maximum electrical heating power is 22.4 kW. With a rod diameter of $d_r = 8.2$ mm the resulting maximal power density is about 100 W/cm². Analysing the velocity profiles, $z_h^* = z_h/d_h$ with z^* referring to the length of the cylindrical rod is chosen instead of z_T^* .

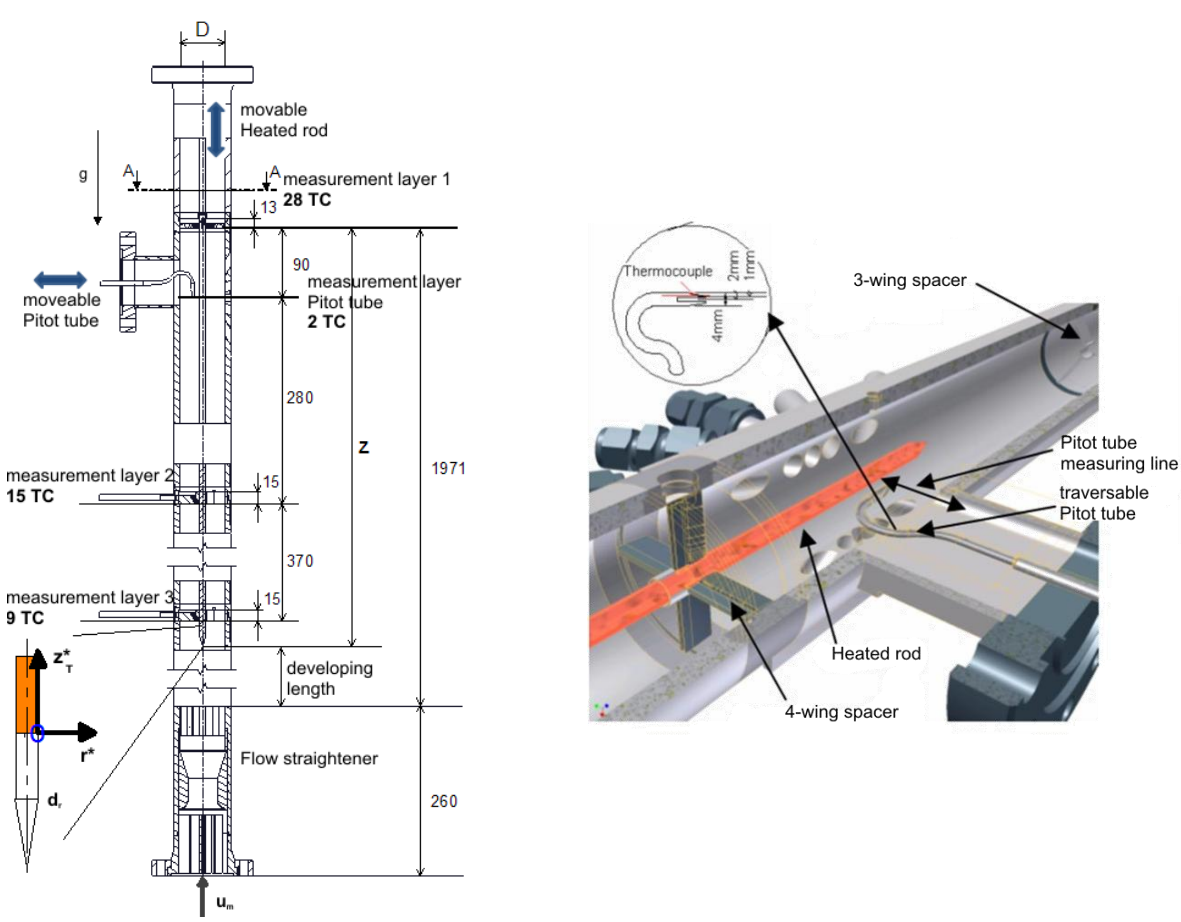


Figure 2: Schematics, used coordinate system and dimensions (in mm) of the single rod experiment and the measurement positions (left); arrangement of the sensor in the experiment (right).

Three equidistant spaced supports (370 mm) ensure the concentric arrangement of the rod in the inner tube. At operating conditions of 300 °C the mean gap between the rod and the

support's tube ring is 0.15 mm. The two lower measurement layers (ML2 and ML3) have three wings; the upper spacer (ML1) has four wings. Sixty calibrated thermocouples (TC), with an outer diameter of 0.25 mm, are mounted on the wings. Each TC is located 1 mm upstream of the wing tip to minimize a potential misreading by upstream heat conduction through the wing material. The wing tip thickness is 1 mm in the flow facing direction and increases up to 2 mm to house all TC and wiring. It is polished to provide a hydraulically smooth surface. In the centre of the wing a tube ring is mounted 5 mm downstream to fix the rod position. A moveable Pitot tube (TP) with an inner orifice of 0.5 mm is located between the second and the third spacer. It is equipped with two thermocouples arranged 0.5 mm upstream of the orifice to enable a simultaneous measurement of temperature and pressure from which the local velocity is deduced.

In order to break the secondary flow induced by a 90° bend, a flow straightener consisting of wings, a venturi tube and a grid array of single tubes (length 100 mm, diameter 10 mm) are installed upstream of the test section. These are followed by a developing length of about 30 hydraulic diameters (L_{dev} =30 D) to ensure a hydrodynamically fully developed flow at the annular test section inlet.

A thermal isolation is wrapped around the test section to minimize heat losses and a specially designed lambda sensor facilitates the control of the oxygen content in the LBE to ensure constant thermal-physical liquid properties. The flow rate is measured by four physically different flow meters, i.e. an electro-magnetic frequency flow meter, a vortex flow meter, a differential pressure measurement and a permanent magnet. The accuracy of the flow rate measurement has been calibrated to ± 0.3 %, which is additionally confirmed by a heat balance calculation. The flow rate oscillation is of the same order of magnitude. During the experimental runs, the long term loop temperature stability is better than ± 0.1 K.

3. Results

3.1 Velocity Profile for Forced Convection

As already stated in literature [10, 12, 14], in the turbulent regime, the location of the maximum in the velocity differs from the location of the zero in the total shear stress as well as from their common location in laminar duct flow. The dimensionless axial velocity u^+ is calculated separately for the inner and outer region of the annulus and the wall shear stresses τ_w can be determined according to [14]. The dimensionless distance from the wall y^+ may be calculated separately as well:

$$u_i^+ = \frac{u}{\sqrt{\tau_{wi}/\rho}} \text{ and } u_a^+ = \frac{u}{\sqrt{\tau_{wa}/\rho}},$$

$$y_i^+ = \frac{y\sqrt{\tau_{wi}/\rho}}{v} \text{ and } y_a^+ = \frac{y\sqrt{\tau_{wa}/\rho}}{v}.$$
(1)

Since the properties of LBE prevent the applicability of measuring techniques such as optical methods (e.g. Laser Doppler Velocimetry (LDV) or Particle Image Velocimetry (PIV)), an increased error with decreasing distance of the Pitot tube from the heated rod has to be accepted (<u>Figure 3</u>). Therefore, neglecting the distortion of the dimensionless velocity profile near the inner rod, the independence of the profile from the applied heat flux has been stated for Re=2.37x10⁵. In the outer region the velocity profile shows very good agreement with the

theoretical profile of van Kármán for tubes [15] as well as with the numerical calculations of Kaneda et al. [14] for pure forced convection in annuli (<u>Figure 4</u> and <u>Figure 5</u>).

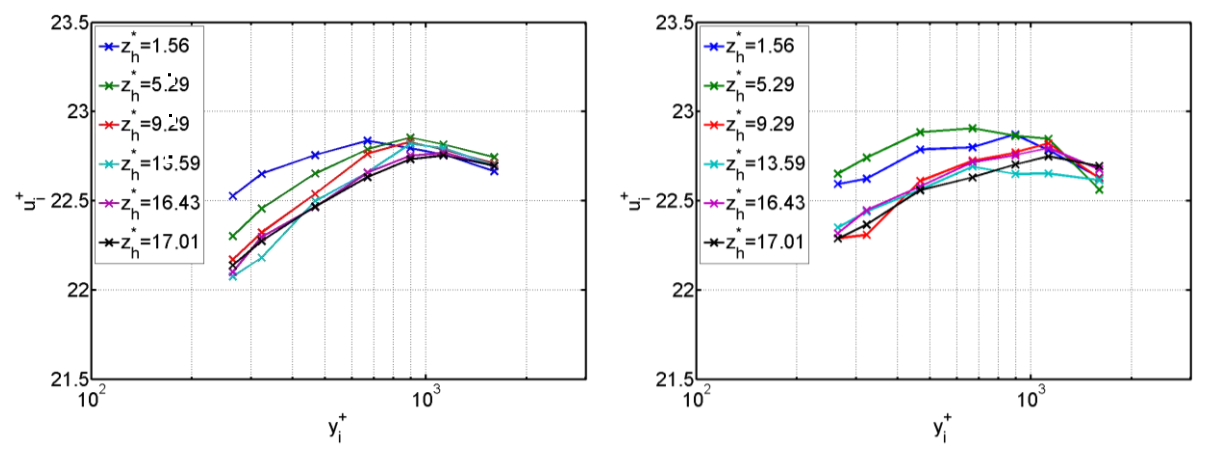


Figure 3: Dimensionless velocity profile for the inner region of the annulus for Re=2.37x10⁵; Q=0 kW (left) and Q=20 kW (right)

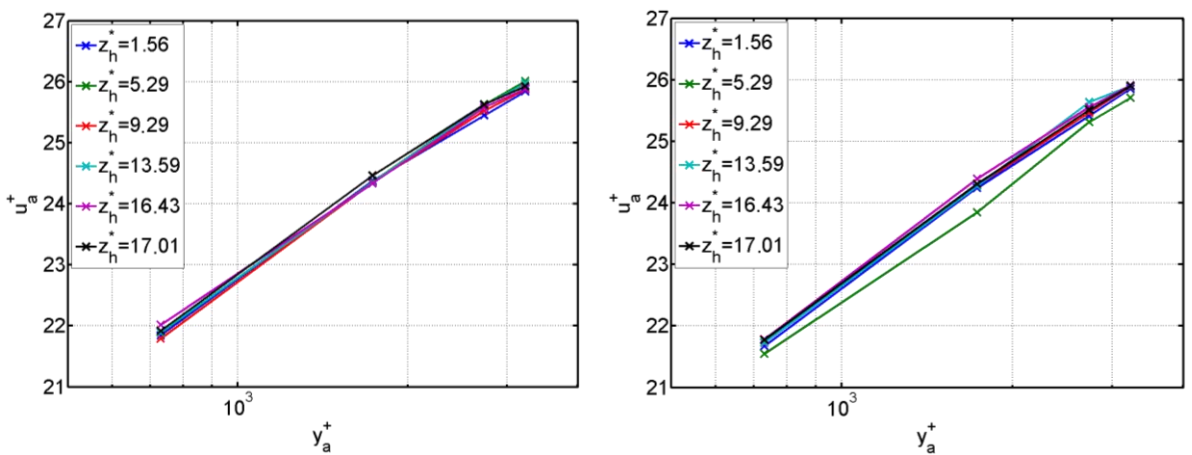


Figure 4: Dimensionless velocity profile for the outer region of the annulus for Re=2.37x10⁵; Q=0 kW (left) and Q=20 kW (right)

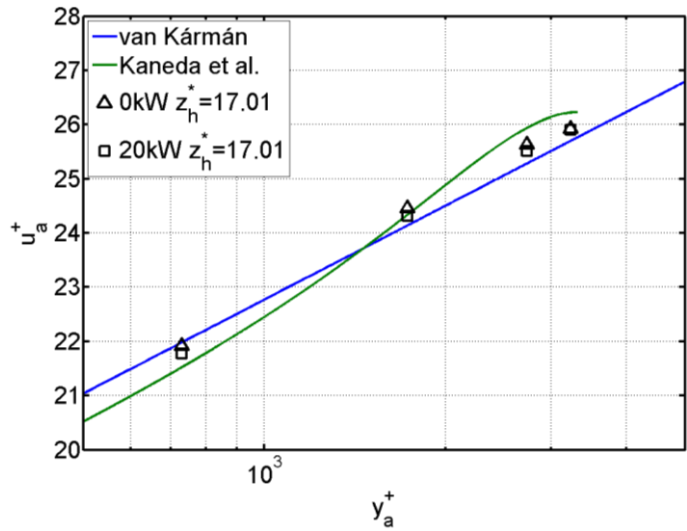


Figure 5: Comparison of experimental results with literature data for the outer region of the annulus ($Re=2.37x10^5$)

3.2 Temperature Profile for Forced Convection

Since the geometric setup is quite complex in most cases and additionally the Reynolds numbers are large, numerical simulations frequently use a Reynolds-averaged Navier- Stokes equations (RANS) approach. Hereby, the turbulent heat fluxes are mostly applied inadequately by a constant turbulent Prandtl number. In this context Baumann et al. [20] compared different advanced models and analyzed them with experimental and Direct Numerical Simulation (DNS) data which are conceived as validated. It appeared the need to adjust the inaccuracy of the turbulence model by altering the Pr_t correlations for the respective shear flow type and the turbulence model.

Exemplary, the validation of the presented heated rod experiment for forced convection (Figure 6) showed a better agreement with the temperature profiles using the Launder-Sharma turbulence model [21] and a constant Pr_t in comparison to the enhanced models such as the empirical equation of Kays [22]. A possible explanation is the too low modeled turbulent viscosity near the rod. More details of the numerical simulations may be taken from [20].

The experimental results exhibit small deviations but generally show a slightly better turbulent mixing than predicted by the simulations. Since neither the mentioned 90° bend prior to the test section nor the flow straightener has been included in the simulated geometry [20], this indirectly indicates the presence of secondary flow which also influences the temperature profile. Additionally a slightly asymmetric velocity profile despite of the flow straightener, was shown in earlier numerical simulations of Batta [23], but could not be determined directly with experiments because the Pitot tube only facilitates velocity measurements of axial velocities at one circumferential position.

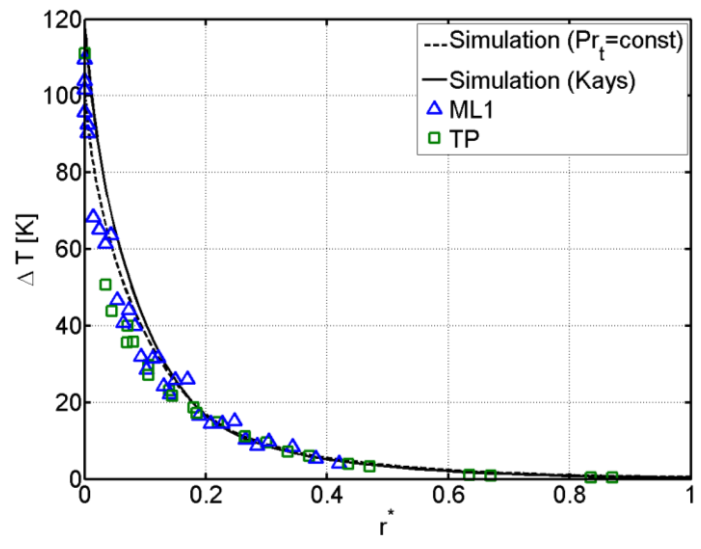


Figure 6: Comparison of measured and calculated temperature profile for Q=20 kW and $z_T*=15.87~(Re=2.37x10^5)$

3.3 Heat Transfer Correlation for Forced Convection

The wall temperatures along the heated rod were either calculated using the measured temperature profiles or directly measured temperature readings conducted by two thermocouples (HT) embedded in the surface of the heated rod. Taking into account the local adiabatic mixing temperature, which was determined by a simple heat balance, the

corresponding Nusselt numbers can be computed. Herein the fluid properties are based on the adiabatic mixing temperature and have been applied according to the correlations from [25].

A comparison of the results of the different measurement techniques shows good agreement except for small z^* (Figure 7), which can be explained with the presence of a secondary flow in the initial region. A selection of the most promising empirical and theoretical heat transfer correlations for low Prandtl number fluids as well as different equations describing the thermal entrance effects, all to be found in literature, were compared with the measured data. The well-known large scatter of the literature data became immediately visible. Therefore only two correlations, namely the one of Dwyer [16, eq. 2] for annuli and the one of Chen and Chiou [6, eq. 4] for tubes and adapted to annuli, were found to be in good agreement with the present data. The promising correlation of Yu et al. [17] exhibits a deviation of 30% although it is based on the theoretical work of [14]. This noteworthy difference is mainly caused by the choice of the simple but imprecise equation of Jischa and Rieke [25] to describe the turbulent Prandtl number.

$$Nu_{\infty,Dwyer} = \left(4.63 + \frac{0.686}{b}\right) + \left(0.02154 - \frac{0.000043}{b}\right) \cdot \left(\overline{\Psi} \cdot Pe\right)^n$$
 (2)

$$\overline{\Psi} = \left(1 - \frac{1.82}{\Pr(0.0185 \operatorname{Re}\sqrt{f_{wm}})^{1.4}}\right), \quad n = 0.752 + \frac{0.01657}{b} - \frac{0.000883}{b^2}$$
(3)

Herein b is the aspect ratio of the annulus, whereas f_{wm} represents the averaged fanning friction factor.

$$Nu_{\text{co-Chen and Chiou}} = 5.6 + 0.0165Pe^{0.85} Pr^{0.01}$$
(4)

In addition, a new empirical equation to describe the thermal entrance effects of low Prandtl number fluids based on the present experiments is introduced:

$$\frac{Nu_z}{Nu_\infty} = 1 + 1.14 \left(\frac{d_h}{z}\right)^{\frac{1}{2}} \tag{5}$$

With the new proposed correlation, the experimental data are within 20% (Figure 7, dotted black line) over almost the whole range of z_T^* . It exhibits an averaged deviation of 6.5% or 5% when using Nu_∞ according to Chen and Chiou (Eq. 4) or Dwyer (Eq. 2 and 3) respectively.

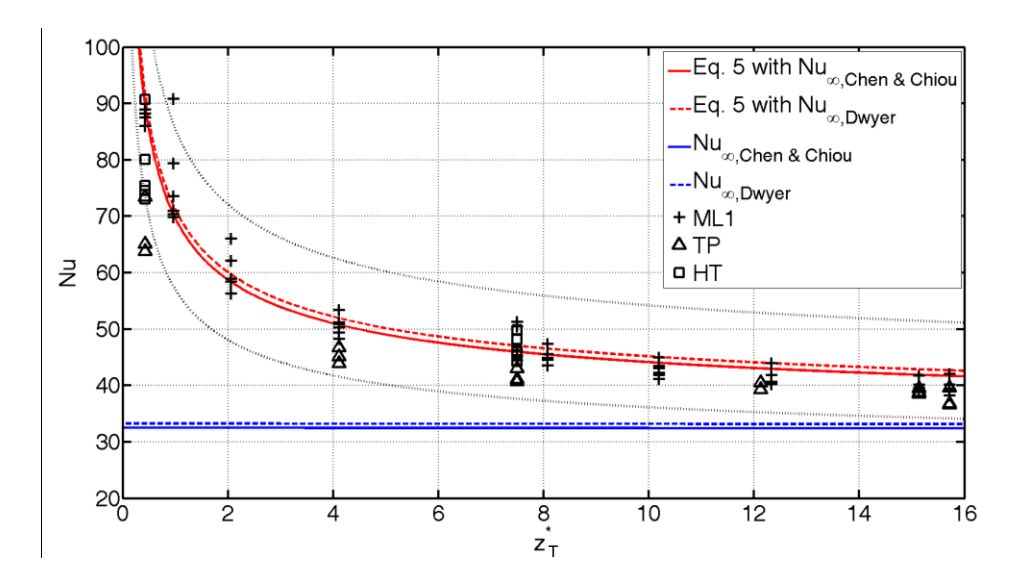


Figure 7: Measured Nusselt number as a function of z_T^* in comparison with the modified Nu correlations based on extension given by eq. (5)

3.4 Transition to Mixed Convection

The large molecular heat conductivity of liquid metals strongly influences the transition from forced to mixed convection. Here the laminarization of the turbulent flow causes a characteristic decline of the heat transfer coefficient. A further increase of the buoyancy forces overrides the laminarisation by accelerating the fluid in the region close to the wall thereby enhancing the heat transfer again.

As a result of experimental investigations with mercury (Hg) and the NaK-eutectic, Buhr et al. [26] suggested the parameter Z (Eq. 6) to estimate the transition from a thermally fully developed vertical forced convective pipe flow to mixed convection. According to [26], free convection effects are not significant below the value of $Z=20x10^{-4}$.

$$Z = \frac{Ra^*}{\text{Re}} \frac{d_h}{L} \tag{6}$$

with

$$Ra^* = Gr^* \cdot \text{Pr} \text{ und } Gr^* = \frac{d_h^3 \cdot \beta \cdot g}{v^2} \frac{dT}{dz} d_h$$
 (7)

In the present study neither distortion of the temperature field nor changes in the velocity field took place at $Re=2.37\times10^5$ for any applied heat flux. However, the calculated values of Z should already indicate significant influence of free convection effects (<u>Table 1</u>). Reason may be found in the different experimental assembly (tube vs. annulus), which limits the applicability of this criterion.

Table 1: Criteria Z (10⁻⁴) according to Buhr [10]

		` /	
Q	$Re=2.37x10^5$	Re=1.18x10 ⁵	Re=5.91x10 ⁴
3kW	24.77	81.60	273.95
9kW	62.48	210.32	746.63
20kW	121.26	438.48	1674.20

In <u>Figure 8</u> the local Nusselt number Nu_{z^*} for mixed convection is related to the local Nusselt number calculated for pure forced convection $Nu_{z^*,fc}$ (according to eq. 5 with Nu_{∞} from Dwyer) at the same Reynolds number and plotted versus the parameter c^* (Eq. 8). Herein the Rayleigh number is based on the wall heat flux and accounts for the buoyancy forces. The Reynolds number resembles the inertial convective forces.

$$c^* = \frac{Ra^{0.333}}{Re^{0.8} Pr^{0.4}}$$
 (8)

For pure forced convection the ratio $Nu_{z^*}/Nu_{z^*,fc} = 1$, for interacting buoyany effects the ratio facilitates the estimation of the heat transfer compared to the case of pure forced convection. The presented data (Figure 8) exhibit a mixed convection zone in the range of approximately $0.09 < c^* < 0.9$, which is stretched compared to O(1) Prandtl number fluids [19]. The large scatter of experimental results at low Reynolds numbers complicates the interpretation for the case of natural convection. The aspect of axial conduction needs to be taken into account as well and cannot be neglected a priori. Nevertheless it can be observed that the gradient of the line representing natural convection decreases with decreasing Prandtl number [27].

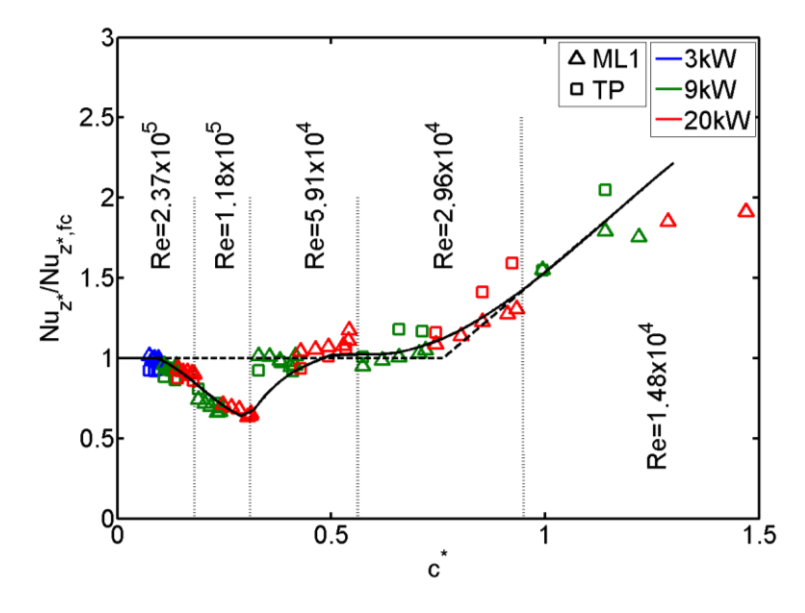


Figure 8: Ratio of the measured to the forced convective Nusselt number in the heated rod experiment as a function of c*, indicating the transition from forced to mixed and eventually natural convection

4. Conclusion

The present paper shows a comparison of measured and computed velocity and temperature distribution of a turbulent flow along a uniformly heated rod concentrically placed in a circular duct.

Despite the defects of liquid metal instrumentation, especially for near wall velocity measurements, a reasonable agreement between prediction and experimental observation is obtained. The results of temperature measurements exhibit an acceptable agreement with simulation data although being aware of deficits in both measurement and simulation. Since different measuring techniques resulted in very similar wall temperatures, a high quality of the experimental setup and high reproducibility of the data could be demonstrated.

A new empirical correlation for the Nusselt number to describe the heat transfer in both a thermally and hydrodynamically developing flow is proposed. In reference to the experimental data the correlation exhibits a considerable improvement compared to the prior status for liquid metal flows.

Furthermore the transition from forced to mixed and natural convection has been analyzed. It could be shown by the experimental data that the mixed convective flow regime differs significantly from O(1) Prandtl number fluids and a new detailed characterization has been proposed.

5. Acknowledgement

The work is supported in the framework of the IP-EUROTRANS project; contract number FI6W-CT-2004-516520.

6. References

- [1] J.U. Knebel et al., "Thermalhydraulic and material specific investigations into the realization of an accelerator driven system (ADS) to transmute minor actinides". Status Report, Forschungszentrum Karlsruhe, FZKA 6506, 1999.
- [2] V. Baylac-Domengetroy, "Investigation related to the generation of reaction products in the target of accelerator driven systems for nuclear waste incineration". Forschungszentrum Karlsruhe, FZKA 6908, 2003.
- [3] J. Zeininger, "Turbulenter Wärmetransport in flüssigem Blei-Bismut an einem vertikalen Heizstab im Ringspalt". PhD Thesis, Universität Karlsruhe (TH), 2009.
- [4] R.C. Martinelli, "Heat transfer to molten metals", Trans. Am. Soc. Mech. Engrs., Vol. 69, 1947, pp.947-959.
- [5] R.N. Lyon, "Liquid metal heat transfer coefficient", Chemical Engineering Progress, Vol. 47, 1951, pp.75-79.
- [6] C.-J. Chen, J.S. Chiou, "Laminar and turbulent heat transfer in the pipe entrance region for liquid metals", International Journal of Heat and Mass Transfer, Vol. 24, 1981, pp.1179-1189.
- [7] Q. Rensen, Experimental investigation of turbulent heat transfer to liquid sodium in the thermal entrance region of an annulus, Nuclear Engineering and Design, Vol. 68, 1981, pp.397-404.
- [8] H.A. Johnson, J.P. Hartnett, W.J. Clabaugh, "Heat transfer to molten lead-bismuth eutectic in turbulent pipe flow", Journal of Heat Transfer, Vol. 75, 1953, pp.1191-1198.
- [9] R.A. Seban, D.F. Casey, "Heat transfer to lead-bismuth in turbulent flow in an annulus", Annual Meeting of the ASME, Paper 56-A-62, 1956.
- [10] K. Rehme, "Turbulente Strömung in konzentrischen Ringspalten". Habilitation, Kernforschungszentrum Karlsruhe, KfK 2099, 1974.

- [11] P.J. Hlavac, B.G. Nimmo, O.E. Dwyer, "Experimental study of effect of wetting on turbulent flow of mercury in annuli", International Journal of Heat and Mass transfer, Vol. 15, 1972, pp.2611-2631.
- [12] S.Y. Chung and G.H. Rhee and H.J. Sung, "Direct numerical simulation of turbulent concentric annular pipe flow Part 1: Flow field", International Journal of Heat and Fluid Flow, Vol. 23, 2002, pp.426-440.
- [13] S.Y. Chung and H.J. Sung, "Direct numerical simulation of turbulent concentric annular pipe flow Part 2: Heat transfer", International Journal of Heat and Fluid Flow, Vol. 24, 2003, pp.399-411.
- [14] M. Kaneda et al., "The characteristics of turbulent flow and convection in concentric circular annuli. Part I. Flow". International Journal of Heat and Mass transfer, Vol. 46, 2003, pp.5045–5047.
- [15] S. Kakac et al., "Handbook of Single Phase Convective Heat Transfer". Wiley, New York, 1987.
- [16] O.E. Dwyer, "Eddy transport in liquid-metal heat transfer", AIChE Journal, Vol. 9, 1963, pp.261–268.
- [17] B. Yu et al. "The computed characteristics of turbulent flow and convection in concentric circular annuli. Part II. Uniform heating on the inner surface". International Journal of Heat and Mass transfer, Vol. 48, 2005, pp. 621–634.
- [18] Heat Atlas, 2nd edition, SpringerVerlag, Berlin-Heidelberg, 2010.
- [19] T. Aicher and H. Martin, "New correlations for mixed turbulent natural and forced convection heat transfer in vertical tubes", International Journal of Heat and Mass transfer, Vol. 40, 1997, pp.3617–3626.
- [20] T. Baumann et al., "Modeling the turbulent heat fluxes in low Prandtl number shear flows", submitted for NURETH 14, Toronto, 2011. September 25-29.
- [21] B.E. Launder and B.I. Sharma, "Application of the energy dissipation model of turbulence to the calculation of flow near a spinning disc", Lett. Heat Mass Transfer, Vol. 1, 1974, pp. 131–138.
- [22] W.B. Kays, "Turbulent Prandtl number where are we?", Journal Heat Transfer, Vol. 116, 1994, pp. 284–295.
- [23] A. Loges, "Untersuchungen zum turbulenten Wärmeübergang im flüssigmetalldurchströmten konzentrischen Ringspalt", MSc. Thesis, KIT, Karlsruhe, Germany, 2010.
- [24] OECD/NEA Nuclear Science Committee, Working Party on Scientific Issues of the Fuel Cycle, Working Group on lead-bismuth eutectic, "Handbook on lead-bismuth eutectic alloy and lead properties, materials compatibility, thermal-hydraulics and technologies", 2007.
- [25] M. Jischa and H.B. Rieke, "About the prediction of turbulent prandtl and schmidt numbers from modified transport equations". International Journal of Heat and Mass transfer, Vol. 22, 1979, pp.1547–1555.
- [26] H.O. Buhr, A.D. Carr, R.E. Balzhiser, "Temperature profiles in liquid metals and the effect of superimposed free convection in turbulent flow". International Journal of Heat and Mass transfer, Vol. 11, 1986, pp.641–654.
- [27] A. Bejan, "Convection Heat Transfer". John Wiley & Sons Inc., 1984.